Accepted Manuscript

Comparison of cutting mechanism when machining micro and nano-particles reinforced SiC/Al metal matrix composites

Xiangyu Teng, Wanqun Chen, Dehong Huo, Islam Shyha, Chao Lin

PII: S0263-8223(18)31461-2
DOI: https://doi.org/10.1016/j.compstruct.2018.07.076
Reference: COST 9994

To appear in: *Composite Structures*

Received Date: 10 May 2018
Revised Date: 10 July 2018
Accepted Date: 17 July 2018

Please cite this article as: Teng, X., Chen, W., Huo, D., Shyha, I., Lin, C., Comparison of cutting mechanism when machining micro and nano-particles reinforced SiC/Al metal matrix composites, *Composite Structures* (2018), doi: https://doi.org/10.1016/j.compstruct.2018.07.076

Comparison of cutting mechanism when machining micro and nano-particles reinforced SiC/Al metal matrix composites

Xiangyu Teng[1], Wanqun Chen[1], Dehong Huo[1, 3*], Islam Shyha[2], Chao Lin[3]

[1]Mechanical Engineering, School of Engineering, Newcastle University, Newcastle upon Tyne, NE1 7RU, UK

[2]Department of Mechanical and Construction Engineering, Northumbria University at Newcastle; Newcastle upon Tyne, NE1 8ST, UK

3The State Key Laboratory of Mechanical Transmission, Chongqing University, Chongqing 400044, China

*Corresponding author: D. Huo, Tel: +44 (0) 191 208 6230, E-mail: dehong.huo@newcastle.ac.uk

Abstract:

Recently, metal matrix composites (MMCs) reinforced with nano-particles receive increasing attention from academia and industries. The cutting mechanism of nano MMCs is believed to be different when compared to composites reinforced with micro particles. This paper presents cutting mechanism comparison between SiC/Al metal matrix composites (MMCs) reinforced with micro and nano-particles using finite element method. The cutting mechanisms are investigated in terms of the von Mises stress distribution, tool-particles interaction, chip formation mechanism and surface morphology. It is found that the particles in nano size remained intact without fracture during the cutting process and are more likely to produce continuous chips, while the particles in micro size are easy to break and tend to form discontinues chips. Better machined surface quality with less defects can be obtained from nano size reinforced MMCs compared with their micro size counterparts. The model validation was carried out by conducting machining experiments on two types of MMCs and good agreements are found with the simulation results.

Keywords: Metal matrix composites; Nanocomposites; Cutting mechanism; Chip formation; Finite element model; Machining

1. Introduction

Like all composites materials, metal matrix composites consist of two or more constituents with different physical, mechanical and chemical properties. Conventional MMCs reinforced with micro-sized particles provide superior mechanical properties such as high specific strength and stiffness, excellent wear resistance and low coefficient of thermal expansion, which make them excellent alternatives to conventional metals in various engineering applications [1,2]. MMCs components are typically fabricated in near net shape process such as casting and forging. But machining processes are indispensable in order to achieve high dimensional accuracy and complex shapes. The strengthening mechanism such as grain reinforcement strengthening, load transfer strengthening, which is attributed to addition of hard particles produce desirable properties which are significantly superior to either of the individual phases [3–5]. As results, the enhanced mechanical properties of MMCs and tool-like hardness of reinforced particles bring challenges to machining process. The

deteriorative machined surface finish and excessive tool wear have been recognised as the main obstacles during machining of MMCs due to their heterogeneous and abrasive nature [6,7].

Some restriction of conventional micro MMCs in specified applications were discovered due to the sacrifice in ductility caused by the large volume fraction of particles when compared to their matrix material [8,9]. In recent years, MMCs reinforced with nanoparticles receive increasing attention in both academia and industries. It was noticed that the MMCs reinforced with small volume fraction of nano-sized particles are found to exhibit even better mechanical properties and temperature creep resistance than those reinforced with larger volume fraction of micro-sized particles without compromising in ductility [10]. Unlike the particle size ranging from 50 to 500 μm in conventional MMCs reinforced with micro particles, the size of particles reinforced within nano MMCs is usually up to 100 nm. Also, in the strengthening mechanism point of view, Orowan strengthening effect plays an important role in strengthening nano MMCs, which is different to that for micro MMCs. Therefore, it is believed that the reduced particles size and volume fraction in nano MMCs will make the machining mechanism different compared with their micro size counterparts.

Various numerical techniques have been used to model the machining process of MMCs in the past two decades. The modelling process can be achieved at two levels, namely macro-mechanical and micro-mechanical models. Within macro-mechanical models, MMCs were treated as macroscopically anisotropic materials without considering fundamental characteristics such as particle size, interface between particles and matrix, particles fracture properties, etc. On the other hand, micro-mechanical models focus on the materials' local behaviours during machining process, and thus they can predict the particles behaviour such as debonding and fracture during tool-particles interaction. Finite element (FE) method exhibits better capability in predicting actual machining characteristics such as the behaviour of matrix and interaction between cutting tool and particles and therefore produces more visible details of materials removal mechanism when compared to experimental approach. As one of the most commonly used numerical approaches, finite element modelling has received growing attention to investigate machining mechanism of MMCs in the past two decades.

Monaghan et al. [6,11] conducted the earliest finite element simulation on machining A356 aluminum alloy based MMCs with 35% volume fraction of SiC particles. They incorporated the equivalent homogeneous material (EHM) models performed by elasto-visco plastic FEA code (FORGE2) into the micromechanical sub-model. This was performed by ANASYS to study the flow stress, interface failure, residual stress and sub-surface damage. Later, a transient dynamic finite element model was established by Ramesh et al. [12] to investigate the diamond turning process of Al6061/SiCp MMCs. They studied the normal and shear stresses field in four different cases, namely tool facing/ploughing aluminium matrix/SiC element respectively, and found that the relative position of SiC element and cutting tool motion produced different magnitudes and patterns in stress. Zhu and Kishawy [13] presented a plane-strain thermo-elasto-plastic finite element model of orthogonal machining of Al6061/Al_2O_3 MMCs. Temperature dependent material properties was incorporated into this simulation. The effective and shear stresses on reinforcements and different machining

deformation zone were investigated. The interface failure model between the matrix material and particles (e.g. particle debonding) was used to explain the formation of tool wear. Although reinforcement was considered in this model, detailed cutting behaviours such as tool-particles interaction and effect of particles on the chip formation process were not simulated. A more detailed investigation considering the tool-particles interaction and its effect on stress/strain distribution within workpiece was firstly conducted by Pramanik et al. [14]. The stress distribution at particles and their surrounding matrix was investigated through three scenarios: particles above, along and below the cutting path and used to explain particles debonding and fracture. Zhou et al. [15] presented a better understanding of particles removal mechanism by studying the von Mises equivalent stress distributed locally within matrix and particle phases. However, their simulation model exhibited an inability to globally simulate the chip formation process and stress/strain distribution under the effect of particles. Later, a multi-step 3D finite element model of production on sub-surface damage after machining of MMCs was provided by Dandekar and Shin [16]. The cutting data obtained from the initial step using equivalent homogenous material (EHM) model was applied to a local multi-phase model. This multi-step method provided an accurate prediction of particle fracture behaviour and the relationship between cutting force and sub-surface damage depth. Recently, Zhou et al. [17] studied the edge defects near the exit of orthogonal cutting by creating a FE model with randomly distributed particles. The brittle fracture of particles and plastic flow of matrix were found in the simulation process which resulted in fragmented chips. The effect of high volume fraction of SiC particles on the high-speed milling process of Al6063/SiC was studied by Wang et al. [18] by establishing a multi-phases two-dimension simulation model using Abaqus/Explicit. The stress distribution in different deformation zone was compared with that in equivalent homogeneous model (EHM). A modeling of the interface between the particles and matrix is essential in order obtain more realistic process outcomes such as tool wear, chip formation, stress/strain distribution and cutting force, etc. Comparative studies were conducted by Umer et al. [19] by developing the heterogeneous finite element models with and without the cohesive zone element when machining Al/SiC. They found that the model with cohesive zone element accurately predicted cutting forces and chip morphology compared to the model without cohesive zone. Later, Ghandehariun et al. [20–22] conducted a series of comprehensive simulation studies by developing micro-mechanical models using cohesive element method. They presented a comprehensive analysis on details of material local behaviours such as tool-particles interaction with effect of cutting speed by incorporating all phases of MMCs including matrix, particles and interface between matrix and particles. Moreover, the plastic deformation in machining of Al6061/Al_2O_3 MMCs was analyzed using adaptive meshing technique to avoid mesh quality deterioration So far, an in-depth investigation on finite element modelling of machining MMCs with micro-size particles has been conducted by previous researchers, but little research can be found on nano MMCs. To fill in this gap, Teng et al. [23] conducted a two-dimensional micromechanical finite element model to simulate micro orthogonal machining of magnesium based MMCs reinforced with nano-sized particles considering the size effect. It was found that, unlike the fragmented chips obtained in machining MMCs with micro-size particles, continuously formed chip with saw tooth appearance was dominant. It is clear that the reduction in particle size could induce significant change in the material removal mechanism.

In this study, simulation models when machining of two types of MMCs reinforced with micro-sized and nano-sized particles were developed respectively. An assumption simplifying the 3D micro milling process to 2D micro orthogonal machining process has been applied in the models. The paper presents a comparison between machining of micro and nano MMCs in terms of stress/strain distribution, tool-particles interaction and machined surface morphology. Finally, validation of FE models was conducted by investigating tool wear, chip morphology and machined surface morphology obtained from micro milling experiment.

2 Finite element modelling procedure

2.1 Model descriptions and experimental validation

In this study, finite element models were developed for machining aluminium based MMCs reinforced with nano-size and micro-size SiC particles respectively. Schematic representation of two models is illustrated in Figure 2. The simulation was performed using ABAQUS/Explicit v6.14-4.

Micro milling experiments were conducted for models validation. Since milling is a complex process, assumptions adopted from Lai et al. [24] on simplifying the three-dimensional (3D) micro milling process to two-dimensional (2D) micro orthogonal process are incorporated. Two assumptions are made:

i. The effect of helix angle on the chip formation and cutting force was ignored, as the axial depth of cut used in the experiment is 30 micrometers which is very small (compared to the tool diameter of 500 μm). Under this condition, the helix angle would make so little effect and hence ignored. Therefore, the 3D milling process is simplified to 2D process.
ii. Another assumption was made for simplifying the 2D milling process to micro orthogonal cutting process. The maximum uncut chip thickness t is less than 4 μm in the model when machining nano MMCs, which is much smaller than the diameter of micro endmill (500 μm) as shown in Figure 1 (a). This large difference between uncut chip thickness and endmill diameter minimise the effect of uncut chip thickness on the cutting process (e.g. cutting force, chip morphology). Thus, it is assumed that the uncut chip thickness is equivalent to that in micro milling process.

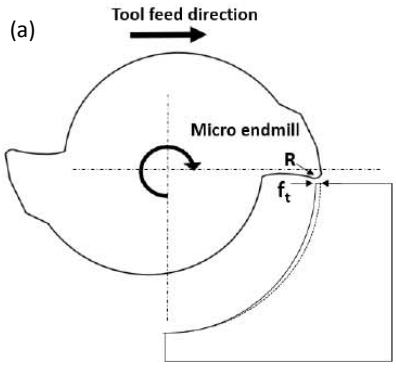

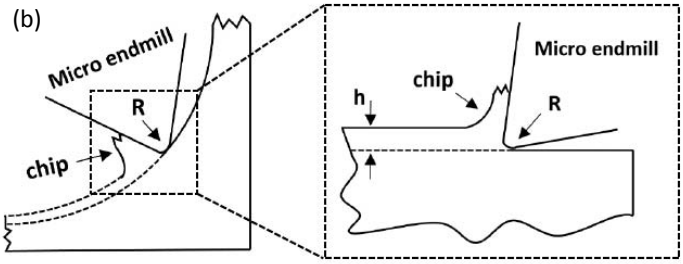

Figure 1. (a) Schematic diagram of 2D milling process in 180° of tool rotation; (b) Relationship between 2D milling process to orthogonal machining process [24].

Microstructure-based two dimensional finite element (FE) models are established. As the large deformation and deformation rate in the workpiece is involved in the cutting process, arbitrary Lagrangian-Eulerian (ALE) formulation with the advancing front algorithm is used to provide the mesh distortion control in every analysis increment to avoid excessive mesh distortion. Free thermal-displacement quad-dominated meshing technique is used to generate mesh. The schematic representation of FE models is shown in Figure 2. For both models, a strategy of particles distribution is established to make the particles distributed at different relative locations of cutting path (see Figure 2). Thus, more realistic models that predict all possible particles behaviours during tool-particle interaction process can be achieved. The cutting tools are treated as analytical rigid body and move horizontally into the fixed workpiece with a predefined speed. The aluminium matrix and SiC particle phases are assigned separately in both models. Two phases are assumed to be perfectly bonded and their interface nodes are tied together. The particle diameter is defined as 200 nm with 10% volume fraction in the nano MMCs model, and 10 μm particle diameter with 10% volume fraction of is used in micro MMCs models. Table 1 lists all machining parameters used in the two models. Due to the scale-difference between two types of reinforcements (nano & micro scale) and the fact that the cutting edge radius of cutting tool is approximately eight times larger than the diameter of nano- particles, it would be computational expensive to apply the same uncut chip thickness in both models. Therefore, different uncut chip thicknesses are used in order to present the typical and distinct tool-particles interaction behaviours.

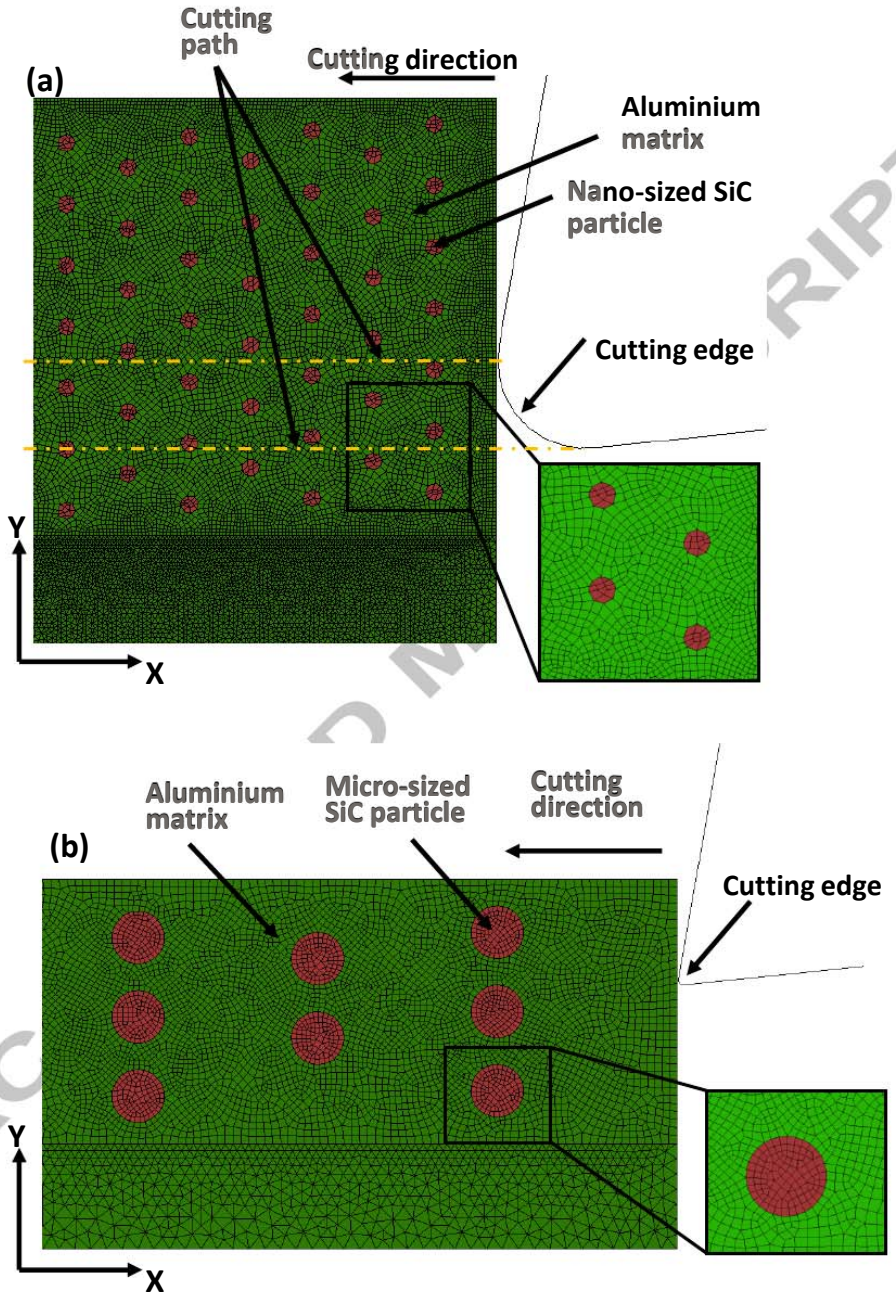

Figure 2. FEA model setup for orthogonal Alinimum based MMCs reinforced with (a) nano-sized SiC particles, (b) micro-sized particles.

For the model of machining nano MMCs, severe deformation of matrix element and large amount of mesh element generated due to the nano sized particles which make the computational process expensive. Therefore, mass scaling option is used to overcome this problem.

Table 1. Machining parameters used in both FE models

Parameters	nano MMCs	micro MMCs
Cutting speed, V_c (m/min)	125.64	125.64
Uncut chip thickness, t (μm)	4	20
Tool rake angle, α (degree)	10	10
Tool clearance angle, β (degree)	6	6
Cutting edge radius (μm)	1	1
Particle size (μm)	0.2	10

The experimental validation was conducted on an ultra-precision desktop micro machine tools (MTS5R). 2-flute uncoated tungsten carbide micro end mills with tool diameter of 0.5 mm were used. The worn end mills, machined surface and chips morphology were examined by scanning electron microscope (Hitachi TM3030).

2.2 Materials properties

Aluminium alloy matrix is assumed to be a deformable thermo-elastic-plastic material with failure criterion in both models. Johnson-Cook (J-C) constitutive equation which is widely used for dynamic problems is used to explore the von-Mises stress distribution during the high speed machining process.

$$\bar{\sigma} = \left[A + B\left(\bar{\varepsilon}^{pl}\right)^n\right]\left[1 + C\ln\left(\frac{\dot{\bar{\varepsilon}}^{pl}}{\dot{\varepsilon}_0}\right)\right]\left[1 - \left(\frac{T - T_{room}}{T_{melt} - T_{room}}\right)^m\right] \quad (1)$$

Where $\bar{\sigma}$ indicates the flow stress, $\bar{\varepsilon}^{pl}$ is the plastic strain, $\dot{\bar{\varepsilon}}^{pl}$ is the plastic strain rate, $\dot{\varepsilon}_0$ is the reference strain rate, T is the workpiece temperature, T_{melt} and T_{room} denote material melting and ambient temperatures. Coefficient A is the yield strength, B is the hardening modulus, C is strain rate sensitivity coefficient, n is the hardening coefficient, m is the thermal softening coefficient. The material constants are normally determined by static tensile test, torsion test and dynamic Hopkinson bar tensile test. Material properties and J-C model parameters for aluminium matrix used in this work are listed in Table 2.

Chip separation criterion of matrix material in the simulated machining process is defined using Johnson-Cook damage equation. The equivalent plastic strain $\overline{\varepsilon_f^{pl}}$ is used as fracture criterion. The failure occurs and the corresponding elements are deleted when damage parameter D equal to unity. The damage parameter D can be defined by:

$$D = \sum \frac{\Delta\overline{\bar{\varepsilon}^{pl}}}{\overline{\varepsilon_f^{pl}}} \quad (2)$$

Where $\Delta\overline{\varepsilon^{pl}}$ is the change of equivalent plastic strain in each integration step. The equivalent plastic strain at the onset of fracture $\overline{\varepsilon_f^{pl}}$ is defined as:

$$\overline{\varepsilon_f^{pl}} = \left(d_1 + d_2 e^{d_3\eta}\right)\left[1 + d_4\, ln\left(\frac{\dot{\varepsilon}^{pl}}{\dot{\varepsilon}_0}\right)\right]\left[1 + d_5\left(\frac{T - T_{room}}{T_{melt} - T_{room}}\right)\right] \quad (3)$$

Where $\dot{\varepsilon}_0$ is the reference strain rate, η is the stress triaxiality, d_1 - d_5 are fracture parameters obtained from tensile and torsion experiments. The reinforcement phase is modeled as a perfectly elastic material. Brittle cracking model available in Abaqus material model library is used to define reinforcement fracture criterion. Mechanical and brittle cracking properties are illustrated in Table 3.

The Coulomb friction model is used to simulate the surface-to-surface contact between cutting tool and workpiece. The friction model is defined as:

$$\tau_{limiting} = \mu\sigma_{contact} \quad (4)$$

$$|\tau| \leq \tau_{limiting} \quad (5)$$

where τ is the equivalent shear stress, $\tau_{limiting}$ is the limiting shear stress, $\sigma_{contact}$ is the normal stress distribution along the rake face and μ is the friction coefficient. During the friction process a sticking region forms between the cutting tool and workpiece and the equivalent shear stress (Equation 4) can be determined by the coefficient of friction μ and normal stress distribution along the rake face σ_n. Once the shear stress at the interface reaches a critical value τ_{lim}, two surfaces will slide relatively to each other. A constant friction coefficient μ =0.5 is used in this simulation.

Table 2. Mechanical properties and materials constant used in J-C model for aluminium alloy

Parameters	values
Density (ton/mm3)	2820×10^{-12}
Young's Modulus (MPa)	70600
Poisson's Ratio	0.35
T_{melt} (K)	900
$T_{transition}$ (K)	290
Thermal expansion (K-1)	23.6×10^{-6}
Thermal Specific Heat (mJ/ton*K)	880×10^{6}
Thermal Conductivity (mW/mm*K)	180
A (MPa)	224
B (MPa)	426
n	0.2
m	0.859
C	0.003
d_1	0.13

d_2	0.13
d_3	-1.5
d_4	0.011
d_5	0

Table 3. Material properties for SiC particles

Parameters	Values
Density (ton/mm3)	3200×10^{-12}
Young's Modulus (MPa)	408000
Poisson's Ratio	0.35
Thermal Specific Heat (mJ/ton*K)	755×10^{6}
Thermal Conductivity (mW/mm*K)	120
Compressive strength (MPa)	3900

3 Results and discussion

Chip formation process when micro machining of Al/SiC MMCs reinforced with nano-sized and micro-sized particles were illustrated in Figure 3 and 4 respectively. The machining characteristics such as chip formation, tool-particles interaction, stress/strain distribution and machined surface defects are investigated.

3.1 von-Mises stress distribution in cutting area

Figure 3(a) and Figure 4(a) show the initial contact stage between the deformed workpiece and cutting tool prior chip formation. Particles distributing at the matrix experiencing with highly concentrated stress zone bear the greatest stress at both models. It proves the fact that hard SiC particles bear most of the load transferred from matrix materials. This can be attributed to the high elasticity of SiC particles. A different phenomenon in terms of von Mises stress distribution pattern within matrix can be found between these two models. When machining nano MMCs (Figure 3a), a narrow straight primary shear zone which can be commonly found in machining homogeneous materials is not obvious. Instead, an irregular highly concentrated stress zone was observed in tool-workpiece interface and the stress from the tool tip progresses to the upper surface with decreasing magnitude. With the cutting tool advances (Figure 3 b&c), a wider primary shear zone when compared to that in machining homogeneous matrix materials (see Figure 5) becomes evident. In contrast, the primary shear zone can be observed when the cutting tool firstly engage with workpiece and lasts during chip formation process in the model of machining micro MMCs (see Figure 4a). The difference in the von Mises stress distribution between the two models implies that the location and size of particles play significant role in determining the stress propagation mechanism with advancement of cutting tool.

In the model of machining nano MMCs, a significant reduction in particle size tends to increase the number of particles involved in the machining area (uncut chip thickness) when

compared to that in machining of micro MMCs. Unlike the highly concentrated stress region confined to the narrow primary shear zone in machining homogeneous materials (see Figure 5), these particles acting as barriers restrict the propagation of stress and force the highly concentrated stress propagate to surrounding area. This is believed to be the main reason leading to an irregular stress zone at tool-workpiece interface at initial cutting stage and wider shear zone with advancement of cutting tool. A detailed study on restricting behaviour of nano-particles is conducted through observing the primary shear zone propagation as shown in Figure 6. With the propagation of primary shear plane, higher magnitude stress attempts to bypass the nano-particle, which in turn causes the irregular stress contour at the interface of each particle. As a result, a fragmented plastic strain field within matrix materials is formed due to the ability of the matrix to deform plastically and particles' inability, see Figure 7. The stress is therefore accumulated near the interface of particles and causes the highly concentrated plastic strain filed.

When the ratio between particle diameter to uncut chip thickness increases, the effect of existence of particle on stress distribution would be more dominated than that in nano MMCs. By observing the von Mises stress pattern in the model of machining micro MMCs, a significant difference when compared to that in machining nano MMCs is that the particle size becomes comparable with the width of primary shear zone (Figure 4b-d). Similarly, micro-particles act as barrier restricting the propagation of primary shear zone. However, the primary shear zone is broken into two regions with the similar area of particle and thus spread to surrounding when it is bypassing the micro particle. Thus, greater compressive stress is generated on the particles under the squeezing action of cutting tool and matrix which results in a concentrated stress zone and maximum plastic strain on the tool-particle interface as shown in Figure 8.

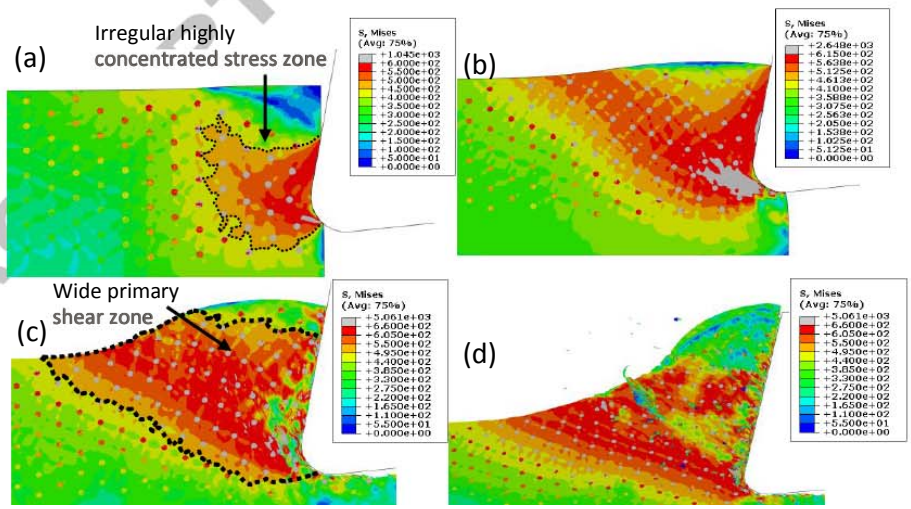

Figure 3. Chip formation when micro machining of Al/SiC MMCs reinforced with nano-sized particles (0.2 μm diameter).

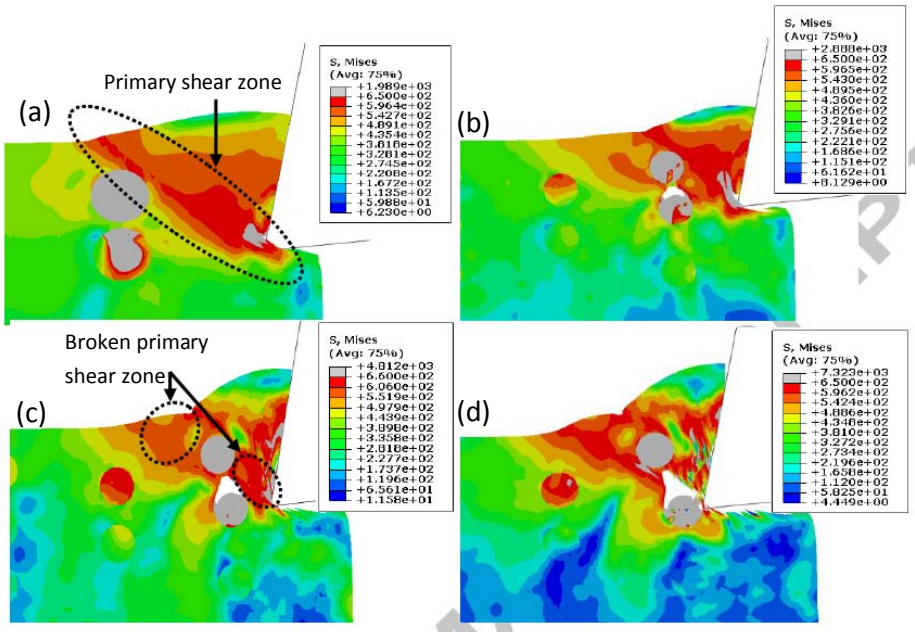

Figure 4. Chip formation when micro machining of Al/SiC MMCs reinforced with micro-sized particles (10 µm diameter).

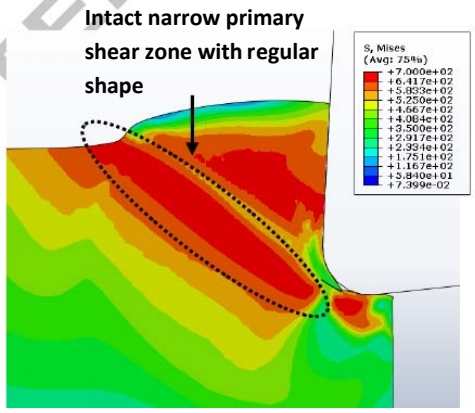

Figure 5. Von Mises stress contour in machining pure Aluminium using the same cutting parameters of nano Al/SiC MMCs machining

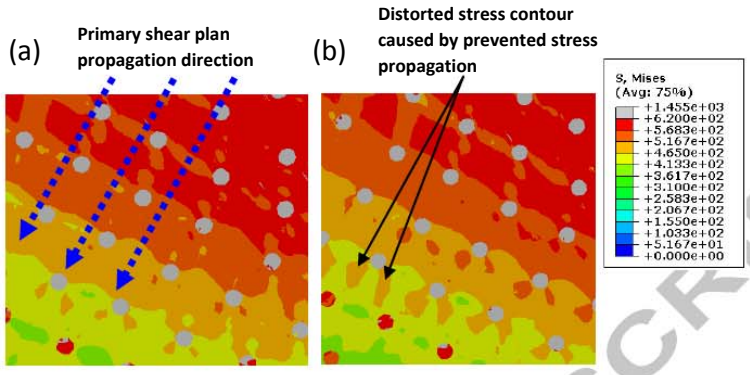

Figure 6. Effect of nano-particles on primary shear zone propagation (a) primary shear zone propagation direction; (b) distorted stress contour caused by prevented stress propagation.

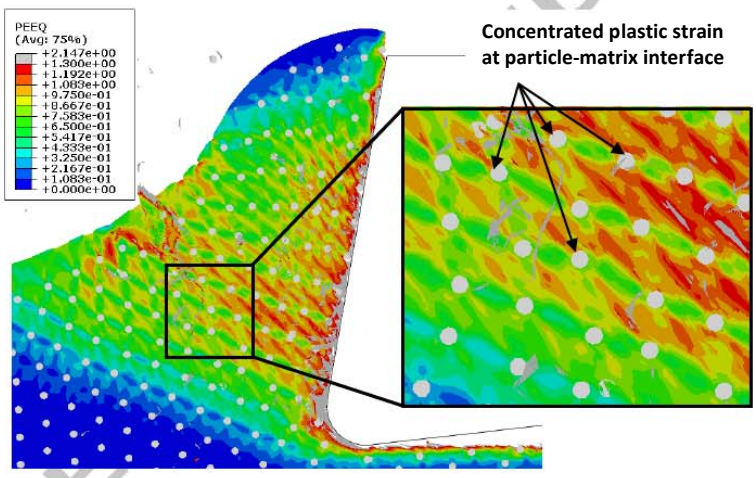

Figure 7. Distorted plastic strain field in machining nano Al/SiC MMCs

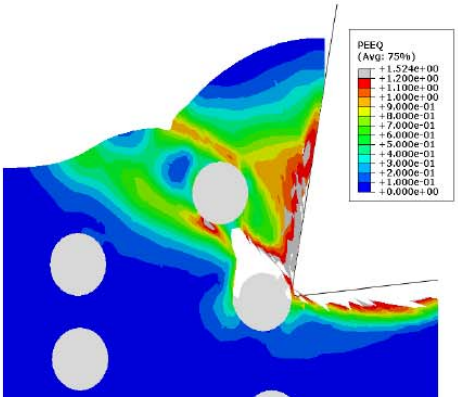

Figure 8. Distribution of plastic strain filed in machining of micro Al/SiC MMCs

3.2 Chip formation process

To analyse the chip morphology characteristics in machining the two MMC materials, it is necessary to understand the stress distribution within matrix. Basically, the size and location of particles play a significant role in the stress distribution pattern in machining process. Figure 9 demonstrates the fragmented chips formation with stress distribution immediately after chip formation shown in Figure 4. Initially, the particles along the cutting path partially deboned without any direct contact with tool tip, see Figure 4 (b). With the tool advances, bypassing of the primary shear plane occurred due to restricting behaviour of particle initiated. Then, a highly concentrated stress zone is formed connecting between the particle interface and upper surface of workpiece in the shear plane and lead to a crack initiation in the matrix as shown in Figure 9 (a). This crack initiation can be further proved by observing the high plastic strain field near this particle in Figure 8 as the MMCs workpiece behaviour in machining is mainly governed by the plastic deformation. As the tool advances, the matrix crack propagates towards the upper workpiece surface as shown in Figure 9 (b). Figure 9 (c) shows the fragmented chips form.

Chips were collected from micro and nano MMCs machining experiments to validate the chip formation models. The increased discontinuity can be observed at the saw tooth structure of the chips obtained from machining of micro MMCs (see Figure 10(a)), whereas continuous chips with saw tooth structure were found in machining nano MMCs (see Figure 10(b)). Same observation was obtained from the experimental work conducted by Teng et al. [23]. It should be noted that although fragmented chips are formed in 2D FE simulation, because the axial depth of cut in the milling experiment is much greater than the micro particle size and also the micro particles are randomly distributed in the matrix, the actual chips may not break along the width of the chip. Therefore, when observing a crossed section of the actual chips, the simulated chips morphology of micro and nano MMCs shows a good consistency with experimental results.

In addition, the highly concentrated stress zone can be found at particle-matrix interface in both models as mentioned earlier. Therefore, it might not be the main reason that lead to fragmented chips in micro MMCs machining process. In fact, the chip formation mechanism in machining micro MMCs is basically depend on the size and location of particles which is the main factor determining the way of stress propagation. By comparing the width of primary shear zone with particle size in these two models, it can be found that the shear zone is keeping intact during chip formation process in nano MMCs rather than being fragmented in micro MMCs. The existence of nano-particle only affect the stress distribution pattern and it does not significantly affect overall integrity of primary shear zone during its propagation. In other words, the restricting behaviour of micro-particles is more dominant than that in nanoparticles, which results in a poor mobility of particles within matrix deformation. This might be due to the large uncut chip thickness to particle diameter in machining nano MMCs. It can be thought that the location of nanoparticles has little effect on the chip formation mechanism in nano MMCs machining process. Therefore, the ratio of uncut chip thickness to particle size might be considered as the fundamental reason determining the chip formation mechanism. Finally, the intact primary shear zone means that the material removal is achieved

by shear sliding in nano MMCs machining process. For micro MMCs, as the result of strong restricting behavior of micro particles, the particle detachment from matrix caused by highly concentrated stress at its interface can be recognised as one of the factors promoting formation of fragmented chips.

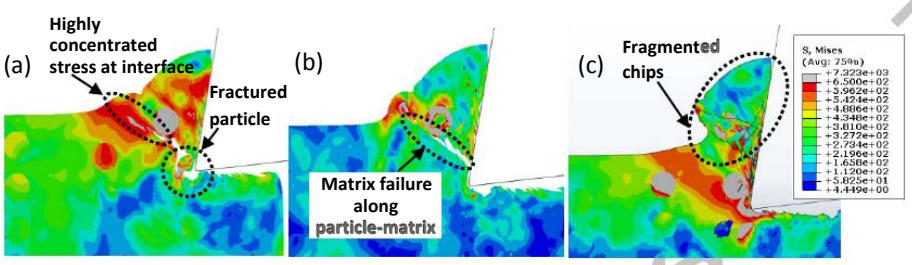

Figure 9. Fragmented chips formation when micro machining of micro Al/SiC MMCs.

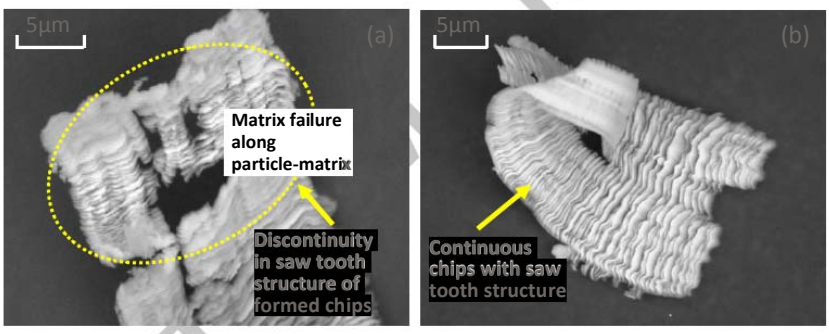

Figure 10. SEM images of chips obtained from machining Al/SiC MMCs reinforced with Vol.10 % (a) micro-sized particles (Φ:10 µm); (b) nano-sized particles (Φ:0.2 µm) under feed per tooth of 4 µm/tooth, cutting speed of 125.64 m/min and depth of cut of 30 µm

3.3 Tool-particles interaction

It is believed that the significant reduction in particle diameter from micro to nanoscale not only influence the chip formation mechanism but also the tool-particle interaction. Figure 11 & 12 illustrate the tool-particle interaction in machining nano MMCs and micro MMCs respectively. It can be observed from Figure 11 that with the formation of continuous chip, the particle embedded within formed chips slides over the rake face generating a high localised stress at the tool-particle contact zone, which is similar as that for micro MMCs. However, the nano-particles are more likely to be squeezed by cutting edge due to theirs significantly large size difference, which leads to a relatively even distribution within particles. Also, the nano-particles exhibit a good mobility within matrix as mentioned earlier. As a result, nano-particles keep intact without cleavage and fracture. In contrast, the micro-particles are observed to experience fracture.

Different behaviours of particle interacting with cutting tool in micro MMCs machining process are shown in Figure 12. It can be seen that the partially debonded particle is embed

within fragmented chips and slide along the cutting tool, resulting in the particle sliding behaviour on the tool rake face and a high localised contact region (see Figure 12 a), which in turn would contribute to the tool wear. The particle located in the cutting path suffers fracture and it was partially imbedded within the newly formed machined surface which might be considered as one of the main factors contributing to surface deterioration (see Figure 12b). Some particles located along or below the cutting path are pressed into the matrix (see Figure 12 (c)). These particles acting as sharp cutting edge lead to the increased residual stress or severe plastic deformation on machined surface. The particle detachment from machined surface leading to the cavity can be observed from Figure 12 (d). This phenomenon is widely acknowledged by previous researchers in both experimental and simulation works.

In addition, the tool particle interaction can be visualised by analysing characteristics of cutting force profile obtained from these two models (see Figure 13). Cutting forces obtained from machining the homogeneous matrix material under the same cutting parameters are also plotted in Figure 13. A larger cutting force fluctuation caused by the tool-particles interaction and fragmented chips formation is observed in micro MMCs machining process when compared to that in homogeneous matrix materials. By comparison, obvious fluctuation in cutting force obtained from machining nano MMCs cannot be observed when compared to that in machining homogeneous matrix. The larger cutting force fluctuation in machining micro MMCs can be explained as results of various tool-particles interaction behaviours and the increased kinetic energy of the large particles.

Generally, the high contact stress at tool-particle interface has been recognised as the main reason causing the tool wear. Various tool wear patterns can be obtained from machining nano and micro MMCs as shown in Figure 14. Tool tip rounding and relatively smooth abrasive wear can be observed on the flank face of the micro endmill in machining nano MMCs (see Figure 14b). This can be attributed to the relatively small size of nanoparticles resulting in a small kinematic energy when compared to micro-particles during tool-particles interaction. In addition, good mobility of nano-particles with matrix deformation is another important factor contributing to the smooth abrasive wear pattern. However, the poor mobility of micro particles within matrix materials and increased kinetic energy of micro-particles are believed to be the main reason that lead to a more severe edge chipping and fracture of tool tip on the endmill used in machining micro MMCs (see Figure 14(a)). Moreover, the unstable and fluctuating nature of machining process caused by different tool-particles interaction behaviours accelerates the wear process as well.

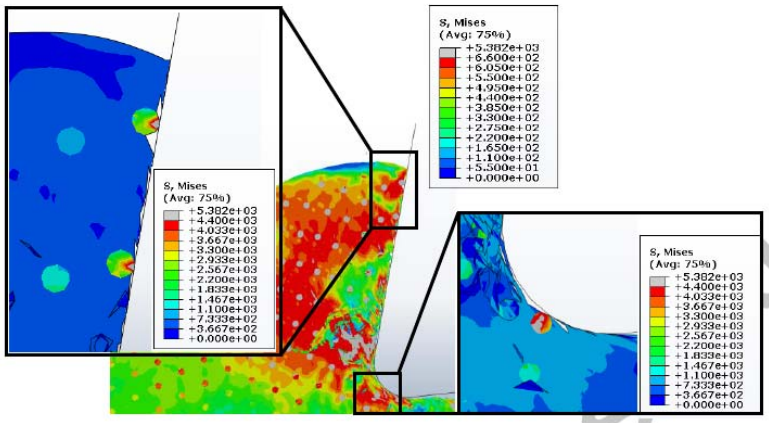

Figure 11. Nanoparticles interacting with cutting tool

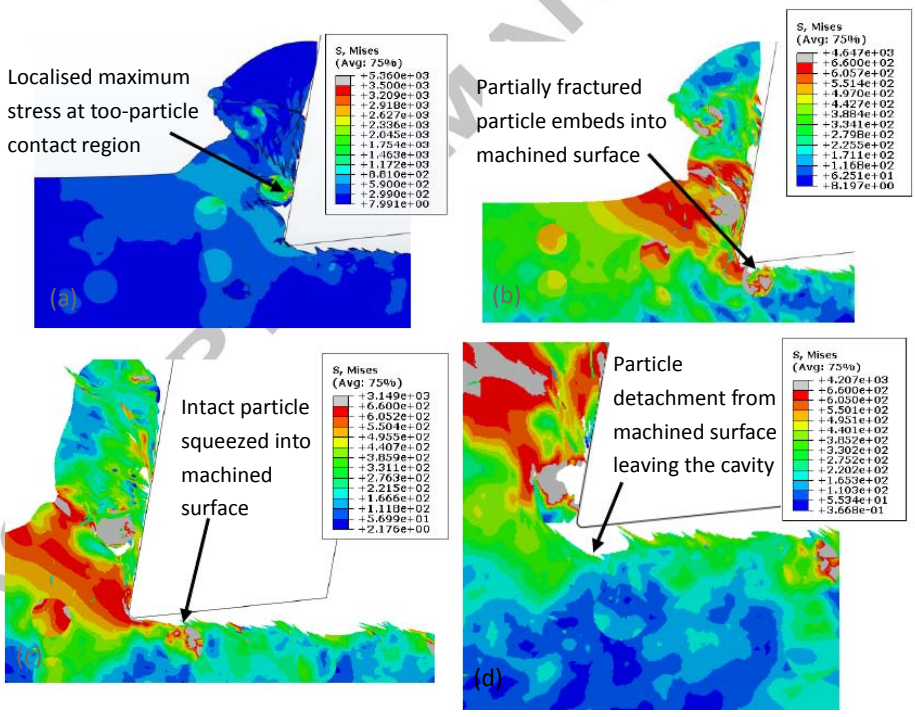

Figure 12. Different tool-particle interaction behaviours in machining micro Al/SiC MMCs.

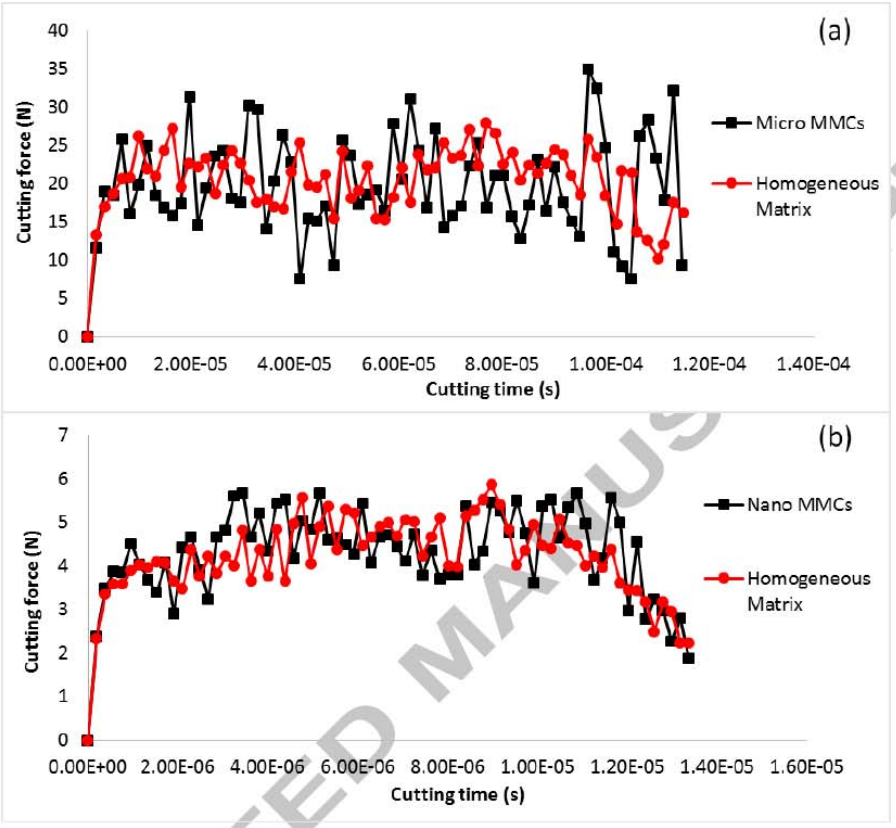

Figure 13. Simulated cutting forces of micro machining Al/SiC MMCs reinforced with (a) micro particles; (b) nano-particles.

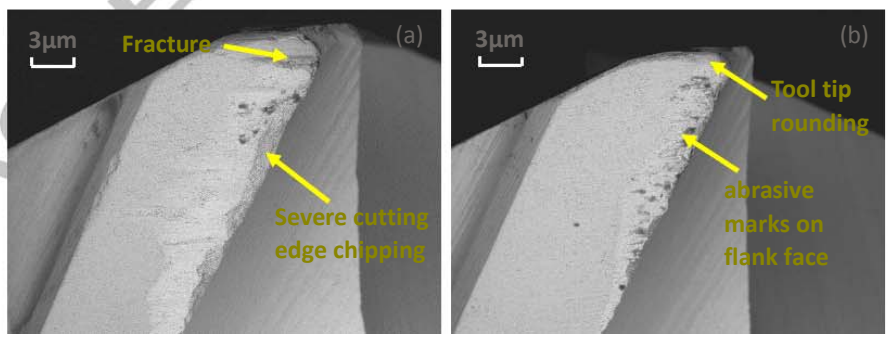

Figure 14. SEM micrographs of main cutting edge wear of micro endmill obtained from machining Al/SiC MMCs reinforced with Vol.10 % (a) micro-sized particles (Φ:10 µm); (b) nano-sized particles (Φ:0.2 µm) under feed per tooth of 4 µm/tooth, cutting speed of 125.64 m/min and depth of cut of 30 µm.

3.4 Machined surface morphology

Different tool-particles interaction behaviours can be found in machining nano and micro MMCs, which in turn leads to different machined surface morphology. Figure 15 shows the simulated surface morphology in machining micro and nano MMCs. The surface deterioration in machining micro MMCs can be attributed to the surface defects such as cavities, scratch marks, fragmented particles embedded within matrix and particles pressed into matrix causing excessive strain, which in turn leads to a matrix failure (see Figure 15 a). The abovementioned phenomenon obtained from simulation model can be easily observed from experimental results. It can be observed from Figure 16 (a) and (b) that the large cavity is formed when the majority of particles located in the cutting path are pulled away from the matrix during tool-particle interaction. Also, the fragmented particle embedded within matrix is observed in Figure 16 (a) which is consistent with simulated results. Excessive compressive stress would be caused by the particles pressed into the machined surface leading to the matrix failure or irreversible plastic deformation. Moreover, during the cutting process, scratch marks on machined surface will be formed when the fragmented particles acting as sharp cutting edge being ploughed through between the flank face of cutting tool and matrix. The magnified images of scratch marks marked in region i and ii can be found in Figure 16 (b). Similar surface morphology can be observed in the simulation model of machining nano MMCs (see Figure 15 b). However, they are not observed in machined surface obtained from experimental works. Distinct milling tool path can be observed on the machined surface (Figure 16 (c). Micro defects can be found at the tool path which broke its continuity. This might be caused by the scratching of residual chips containing nano-particles at the tool-matrix interface during high speed machining. It can be said that the significant reduction in particles size is beneficial for improving the machined surface quality.

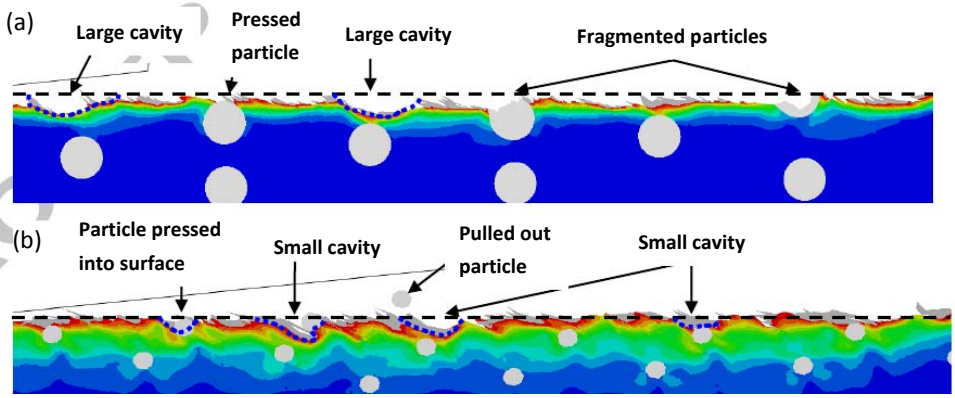

Figure 15. Simulated surface morphology from machining (a) micro MMCs; (b) nano MMCs.

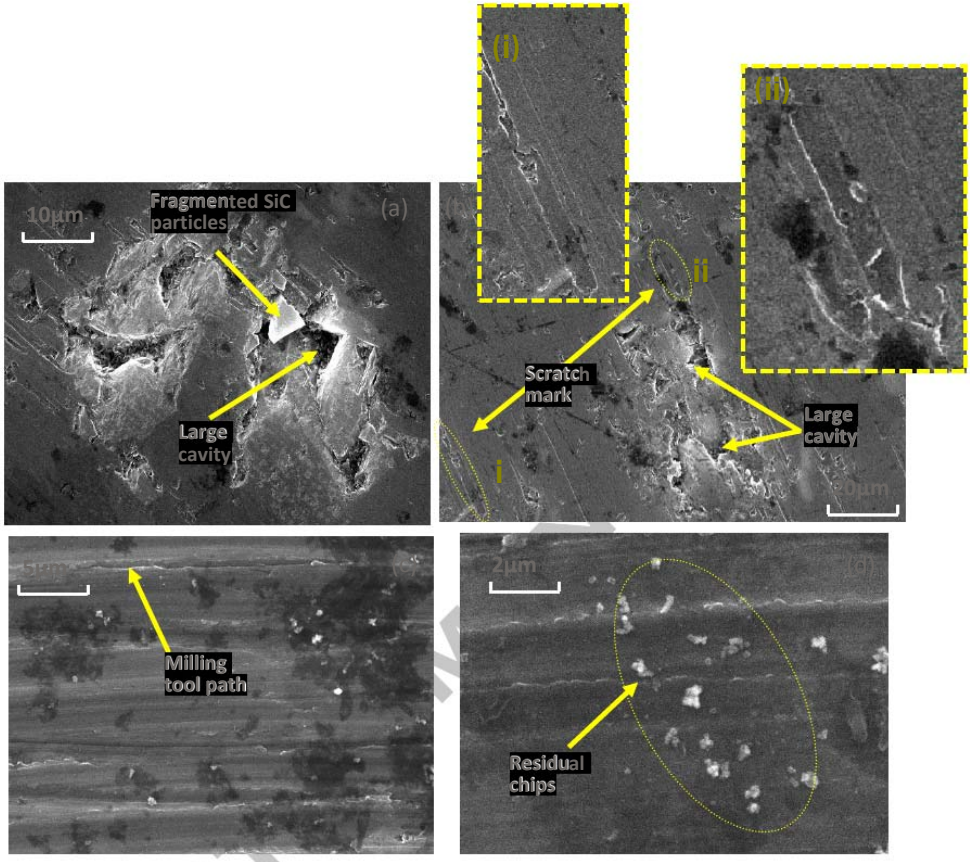

Figure 16. SEM micrographs of machined surface from experimental works (a)&(b) micro MMCs; (c)&(d) nano MMCs under the feed per tooth of 4 µm/tooth, cutting speed of 125.64 m/min and depth of cut of 30 µm.

4 Conclusions:

The following conclusions can be drawn from this paper:

1. The decrease in particle size leading to the different particle restricting behaviors exhibited a significant effect on the stress propagation within workpiece and it was concluded as the main reason causing the various von Mises stress distribution pattern in nano and micro MMCs. The restricting behavior would become more significant with increasing of particle size
2. The stress propagation determined by the ratio of particle size and uncut chip thickness was considered as the main factor determining the chip formation mechanism. In machining of micro MMCs, the size and location of particles play predominant role for chip formation mechanism due to the increased ratio of particle size and uncut chip thickness. In machining of nano MMCs, due to the reduced size, the ratio of uncut chip thickness to particle size might be considered play little effect in determining the chip formation mechanism.

3. The better mobility of nano particles within matrix due to reduced size makes them be squeezed by cutting edge, which in turn produces evenly distributed stress and less kinetic energy on nano particles during machining. This leads to intact particles, which is different from the micro particles showing cleavage and fracture. This observation has been verified by simulated cutting force profile and tool wear pattern obtained from experiments. The way of stress propagation mode within matrix under the effect of particle size is found to determine the chip formation mechanism. Continuous chip formation is observed in machining nano MMCs, while chips obtained from machining micro MMCs tends to be discontinuous.
4. By comparing with the machined surface morphology obtained from machining micro and nano MMCs, it can be concluded that the reduced particle size (nano particles) is beneficial for improving surface quality.
5. Model validation was conducted by comparing the machined surface and chip morphology obtained from simulation model and micro milling experiments and a good agreement was obtained. The assumption for the effect of particles on tool wear has also been verified by observing the worn tool obtained from experiments.

Acknowledgment

The authors wish to thank the Engineering and Physical Sciences Research Council (EP/M020657/1) and Visiting Scholar Foundation of the State Key Laboratory of Mechanical Transmission in Chongqing University (SKLMT-KFKT-201613) for the support for this work.

Reference:

[1] Wang Z, Chen T-K, Lloyd DJ. Stress distribution in particulate-reinforced metal-matrix composites subjected to external load. Metall Trans A 1993;24:197–207. doi:10.1007/BF02669616.

[2] El-Gallab M, Sklad M. Machining of Al/SiC particulate metal matrix composites Part II: Workpiece surface integrity. J Mater Process Technol 1998;83:277–85. doi:10.1016/S0924-0136(98)00072-7.

[3] Miller W., Humphreys F. Strengthening mechanisms in particulate metal matrix composites. Scr Metall Mater 1991;25:33–8. doi:10.1016/0956-716X(91)90349-6.

[4] Taya M. Strengthening mechanisms of metal matrix composites. Mater Trans JIM 1991;32:1–19.

[5] Zong BY, Zhang F, Wang G, Zuo L. Strengthening mechanism of load sharing of particulate reinforcements in a metal matrix composite. J Mater Sci 2007;42:4215–26. doi:10.1007/s10853-006-0674-7.

[6] Monaghan J, Brazil D. Modelling the flow processes of a particle reinforced metal matrix composite during machining. Compos Part A Appl Sci Manuf 1998;29:87–99. doi:10.1016/S1359-835X(97)00047-X.

[7] Ozben T, Kilickap E, Çakir O. Investigation of mechanical and machinability properties of SiC particle reinforced Al-MMC. J Mater Process Technol 2008;198:220–5.

doi:10.1016/j.jmatprotec.2007.06.082.

[8] Ye HZ, Liu XY. Review of recent studies in magnesium matrix composites. J Mater Sci 2004;9:6153–71. doi:10.1023/B:JMSC.0000043583.47148.31.

[9] Mazahery A, Abdizadeh H, Baharvandi HR. Development of high-performance A356/nano-Al2O3 composites. Mater Sci Eng A 2009;518:61–4. doi:https://doi.org/10.1016/j.msea.2009.04.014.

[10] Gupta M, Leong W, Wong E, Properties M. AN INSIGHT INTO PROCESSING AND CHARACTERISTICS OF MAGNESIUM BASED n.d.

[11] Monaghan J, Brazil D. Modeling the sub-surface damage associated with the machining of a particle reinforced MMC. Comput Mater Sci 1997;9:99–107. doi:10.1016/S0927-0256(97)00063-3.

[12] Ramesh M V., Chan KC, Lee WB, Cheung CF. Finite-element analysis of diamond turning of aluminium matrix composites. Compos Sci Technol 2001;61:1449–56. doi:10.1016/S0266-3538(01)00047-1.

[13] Zhu Y, Kishawy HA. Influence of alumina particles on the mechanics of machining metal matrix composites (tie constrains). Int J Mach Tools Manuf 2005;45:389–98. doi:10.1016/j.ijmachtools.2004.09.013.

[14] Pramanik A, Zhang LC, Arsecularatne J a. An FEM investigation into the behavior of metal matrix composites: Tool-particle interaction during orthogonal cutting. Int J Mach Tools Manuf 2007;47:1497–506. doi:10.1016/j.ijmachtools.2006.12.004.

[15] Zhou L, Huang ST, Wang D, Yu XL. Finite element and experimental studies of the cutting process of SiCp/Al composites with PCD tools. Int J Adv Manuf Technol 2011;52:619–26. doi:10.1007/s00170-010-2776-2.

[16] Dandekar CR, Shin YC. Multi-step 3-D finite element modeling of subsurface damage in machining particulate reinforced metal matrix composites. Compos Part A Appl Sci Manuf 2009;40:1231–9. doi:10.1016/j.compositesa.2009.05.017.

[17] Zhou L, Wang Y, Ma ZY, Yu XL. Finite element and experimental studies of the formation mechanism of edge defects during machining of SiCp/Al composites. Int J Mach Tools Manuf 2014;84:9–16. doi:10.1016/j.ijmachtools.2014.03.003.

[18] Wang B, Xie L, Chen X, Wang X. The milling simulation and experimental research on high volume fraction of SiCp/Al. Int J Adv Manuf Technol 2016;82:809–16. doi:10.1007/s00170-015-7399-1.

[19] Umer U, Ashfaq M, Qudeiri JA, Hussein HMA, Danish SN, Al-Ahmari AR. Modeling machining of particle-reinforced aluminum-based metal matrix composites using cohesive zone elements. Int J Adv Manuf Technol 2015;78:1171–9. doi:10.1007/s00170-014-6715-5.

[20] Ghandehariun A, Kishawy HA, Umer U, Hussein HM. Analysis of tool-particle interactions during cutting process of metal matrix composites n.d. doi:10.1007/s00170-015-7346-1.

[21] Ghandehariun A, Nazzal M, Kishawy HA, Umer U. On modeling the deformations and tool-workpiece interactions during machining metal matrix composites. Int J Adv Manuf Technol 2017;91:1507–16. doi:10.1007/s00170-016-9776-9.

[22] Ghandehariun A, Kishawy HA, Umer U, Hussein HM. On tool-workpiece interactions during machining metal matrix composites: investigation of the effect of cutting speed. Int J Adv Manuf Technol 2016;84:2423–35. doi:10.1007/s00170-015-7869-5.

[23] Teng X, Huo D, Chen W, Wong E, Zheng L, Shyha I. Finite element modelling on cutting

mechanism of nano Mg/SiC metal matrix composites considering cutting edge radius. J Manuf Process 2018;32. doi:10.1016/j.jmapro.2018.02.006.

[24] Lai X, Li H, Li C, Lin Z, Ni J. Modelling and analysis of micro scale milling considering size effect, micro cutter edge radius and minimum chip thickness. Int J Mach Tools Manuf 2008;48:1–14. doi:10.1016/j.ijmachtools.2007.08.011.